Indian Journal of Pure & Applied Physics
Vol. 62, December 2024, pp. 1074-1090
DOI: 10.56042/ijpap.v62i12.8069

Thermal Conductivity Enhancement of Phase Change Materials Using Metal Wire Woven Porous Structures for Thermal Energy Storage

Anup Kumar Khare[a,b], Mohit Sharma[a,b]*, Gaurav Kumar Gupta[a,b], Manoj Kumar Gupta[a,b], N Prasanth[b] & Hari N Bhargaw[a,b]

[a]CSIR–Advanced Materials and Processes Research Institute, Bhopal, M.P, 462 026, India

[b]Academy of Scientific and Innovative Research (AcSIR), Ghaziabad, U.P, 201 002 India

Received 25 January 2024; accepted 8 November 2024

In the present work, the thermal conductivity of paraffin wax has been increased using low-cost and lightweight aluminium wire metal foam structures. The designed metal wire foam structures have uniform-sized circular pores forming a convective spring-like network for faster heat transfer. The paraffin wax can easily infiltrate the designed wire woven foam structures even at a lower porosity (~75 vol %). The latent heat thermal energy storage (LHTES) systems which can store up to 500 kJ of thermal energy have been designed using the PCM-wire-woven metal foam composite material. The heating of these composites is carried out both in convection and conduction modes, and their effect has been studied. The effect of using a polymer (acrylic), and a galvanized iron (GI) sheet to encapsulate PCM-metal wire foam composites is also evaluated. Increasing the pore diameters in the wire woven structures, and its effect on the thermal efficiencies of the LHTES system is calculated. The thermal efficiency of the LHTES ranged from 67 to 92 % using an acrylic sheet, and 72 to 77 % using the GI sheet. The heat extraction using cold water could be continued for 8-9 cycles in acrylic, and 5-6 cycles in GI sheet capsulation.

Keywords: Thermal energy; Energy storage; Wire woven metal foam; Thermal conductivity enhancement; Heat and mass transfer

1 Introduction

Phase change materials (PCM) have been researched tremendously during the past decade due to their lower costs than other energy storage techniques like electrical battery systems, mechanical energy storage, *etc*[1]. Phase change materials mostly store the latent heat by their phase transition from solid to liquid phase[2]. The phase change materials have varied applications ranging from building cooling, solar energy storage, solar thermal power plants, textiles, *etc*[3-9]. In one of the categories of PCMs, organic PCMs such as paraffin wax, polyethylene glycol, fatty acids, and, their derivatives are applied in various thermal energy storage applications[3].

Organic PCMs have certain advantages compared to other PCMs as they melt congruently, have large latent heat of fusion, are non-corrosive, thus making them quite attractive for thermal energy storage applications[2,10]. The major limitation of organic PCMs is their lower thermal conductivities[12]. Most of the organic PCMs have low (<1 W/m°K) thermal conductivities and hence their thermal conductivities have to be raised using various thermal conductivity enhancers. Some of the major thermal conductivity enhancers are metal foams, metal fins, nano-powders of high thermal conductivity metals, and graphite, multi walled carbon nanotubes (MWCNT) *etc*[11-15].

Chen *et al.*[16] have shown that the PCMs and high thermal conductive metal foams increase the overall thermal conductivity of PCMs. Siahpush *et al.*[17] used eicosane as the PCM and highly porous copper foam for its thermal conductivity enhancement from 0.423 W/m°K to 3.06 W/m°K. A similar increase was also observed using the aluminium foams[18]. Zhu *et al.*[19] have shown that the smaller pore size has an incremental effect on the thermal conductivity of PCMs. Although, the metal foams with fine pores increase the thermal conductivity but hinder the convection of heat within the system. Therefore, it was suggested in some earlier studies to have fine pores near the heater, and thereafter larger sized pores could be used for faster heat transfer[20,21].

Hu *et al.*[22] have shown numerically that the use of aluminium foams can increase thermal conductivity as well as help in the uniform distribution of heat. They numerically simulated an aluminium foam with uniform square-shaped pores with different pore sizes and porosities. The Al foam (10 PPI) with 70 and 95 % porosity has increased the thermal conductivity

*Corresponding author: (E-mail: mohit826@gmail.com)

of paraffin wax by 123 and 17 times. This increase is much large and can be aneffective solution for the thermal conductivity enhancements of PCM. Similarly, copper foams have also been utilized for the thermal conductivity enhancement of the sodium acetate tri-hydrate salt and its conductivity has also increased to 176 %. To increase the thermal conductivity of the foams, they have also been coated with 3D chemical vapor deposited diamond on the cell walls of the copper foams. The thermal conductivity of the pure paraffin improved to 6.7 W/m°K much larger than pure copper foams[23].

However, it can be pointed out here that the pore shape, size, and density have a major effect on the increase of thermal conductivity. The fine pores have a higher thermal conductivity compared to the coarser-sized pores. However, the fine pores decrease the convective heat transfers due to the reduced space for convective heat transfer. So, it can be understood from the above discussion that the thermal conductivity of the PCMs is increased by using metallic foams. However, it has to be kept in mind that the metallic foams don't restrict the convective channels/paths present throughout the LHTES tank.

In the present work, we have used low-cost convective-designed metal wire foams popularly known as wire-woven cellular materials[24] for the thermal conductivity enhancement of the PCMs. The pores in the wire metal foams have a constant circular shape, are of uniform diameter, and possess a spring-like convective network. The pores a represent uniformly one over the other like a spring structure. This is done to provide convective channels throughout the PCM-metal foam composite.

The lower cost of these wire foams in comparison to the open cellular metal foams used in earlier studies is an added advantage. The cost of the raw material *i.e*. metal wires is low and can be easily fabricated from the wire-woven metal foam structures. The cost of the aluminium wire is approximately 3-4 US$ per kg and even the large metal structures will require only a few kilograms of wire. Hence, the cost of the raw material for making the metal foam structures will be low compared to open cellular foams.

The other advantage of using metal wire is that it itself becomes the strut/cell wall of the foam and is also thick and dense. It has been shown earlier[25] that the thicker and denser struts in metal foams conduct the heat more effectively. The open cellular metal foams used in the earlier works have porous struts due to the processing constraint of using a polymer scaffold. So, it may be assumed that the dense wires may conduct heat in a better way. Further, the effect of increasing pore diameter in the wire foams is also seen and the optimal pore diameter for maximizing thermal efficiency is found in this study. A thermal analysis has also been done to find out the effect of using the metallic and non-metallic encapsulation on the metal wire foam-paraffin wax composites. A thorough analysis of the heat stored in the encapsulated PCM-foam composites has been studied and their thermal efficiencies have also been calculated. An experimental analysis of the obtained temperature profile in the encapsulated boxes during the heating and cooling of the PCM-foam composites is also performed.

2 Experimental Procedure

2.1 Acrylic Box Fabrication

The acrylic sheets were cut and pasted together with the help of an epoxy adhesive with the commercial name Araldite. An acrylic box (Fig. 1(a)) was thus prepared with internal dimensions of 10 x 10 x 13 cm. A similar dimension GI sheet box was also prepared using the sheet metal working and sealed using the epoxy adhesive (Fig. 1(b)).

2.2 Spiral Structure Fabrication

For the fabrication of the spiral structure, an aluminium wire of diameter 1 mm is taken. The aluminium wire is twisted around a 1 meter-long steel rod having 4 mm diameter (Fig. 2(a)).The aluminium wire is wrapped around the steel rod to form an aluminium wire spring with a 4 mm internal diameter. The aluminium spring obtained after twisting has a pitch of 2 mm (Fig. 2(b)). The aluminium wire springs have a free length of 10 cm and 30-35 coils are present in each spring. 250-260 springs were tied together using three aluminium wires to form a rectangular cube of dimensions 10 x 10x 10 cm (Fig. 2(c)). Similarly, by taking steel rods of 5 mm and 6 mm respectively, the aluminium springs with internal diameter of 5 and 6 mm were also made and tied in the form of cubes.

2.3 Heater fabrication

A nichrome wire of 0.1 mm diameter and 4-meter length is used for making the heater coil for DC heating. The nichrome wire heater spring is made by coiling it around a 4 mm diameter steel rod as explained in section 2.2. The nichrome wire heating coil is then engraved in an area of 6.5 x 6.5 cm on a 10 x 10 cm alumina sheet as shown in the Fig. 3. The total resistance of the coil was measured as 138 Ω.

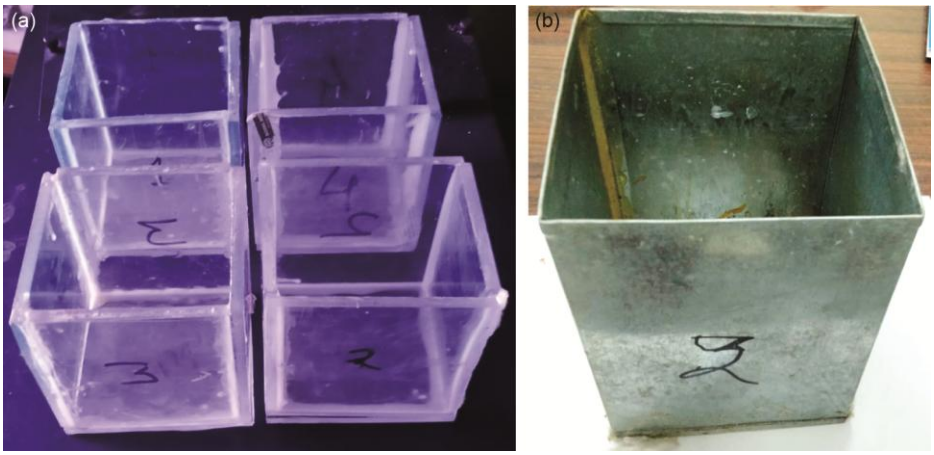

Figure 1 — The encapsulation boxes prepared using epoxy and (a) acrylic and (b) GI sheets, and (c) Stainless steel container

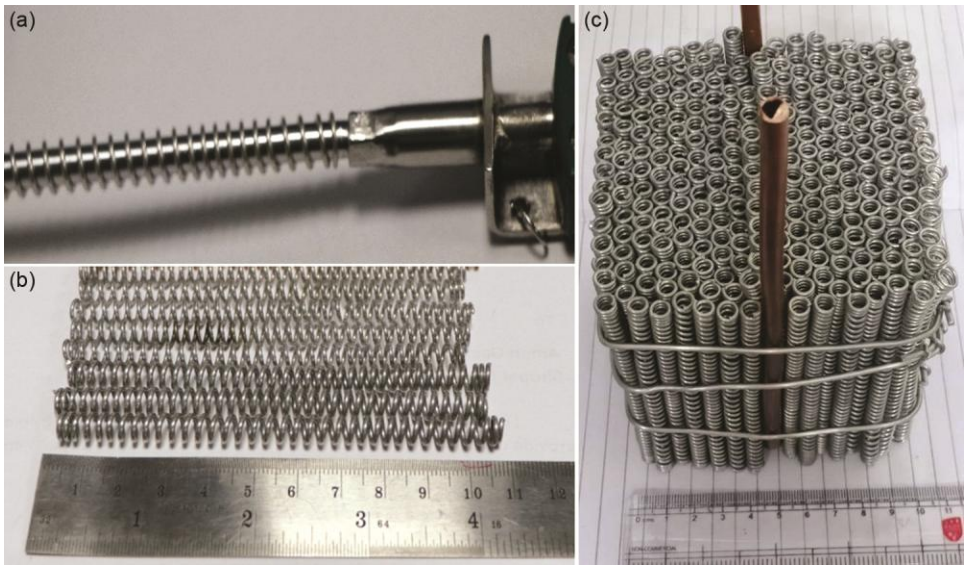

Figure 2 — The preparation method of the wire woven structures with different pore diameters (a) coiling of aluminium wire around the steel rod (b) aluminium wire springs and (c) the coiled aluminium springs tied together to form 10 x 10 x 10 cm cubes

Figure 3 — The heater prepared using the nichrome wire (0.1 mm) spread in an area of 6.5 x 6.5 cm

2.4 LHTES tank fabrication

To start the experiment, a 5 mm diameter copper pipe is fitted onto the aluminium cube foam structure to flow water in such a way that the pipe passes touching the sides and bottom surface of the cube and its ends are outside the encapsulation (Fig. 4(a)). In the front sheet of the encapsulation, 2 mm diameter holes at 0.5cm, 5cm, and 9.5cm respectively from the bottom of the acrylic encapsulation box (Fig. 4(b)). K-type thermocouple is placed in all three holes to measure the temperatures in the box. After drying the box, the spiral foam structure cube is placed and after which the paraffin wax is placed in the box and put in such a way that the wax fills the encapsulated box. After this, the wax was allowed to cool for a day and during each stage, the mass of the box was determined.

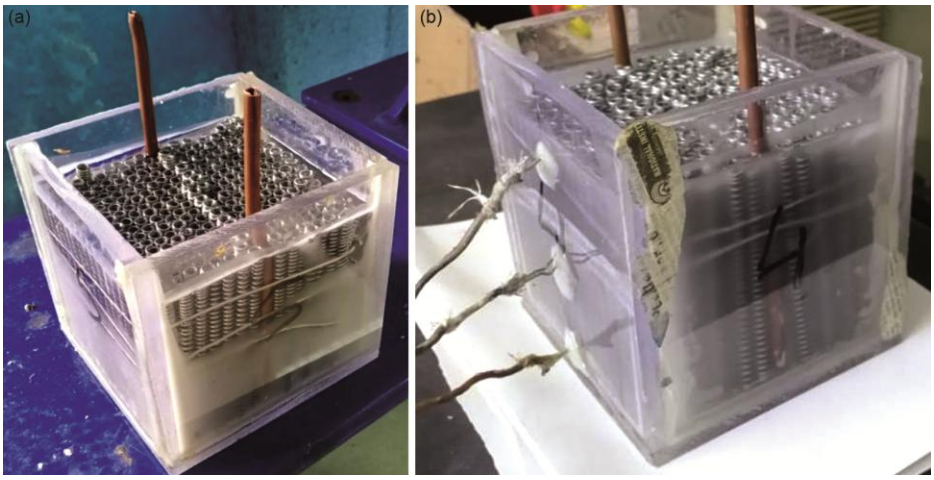

Figure 4 — The LHTES tank filled with the wax, wire woven metal foams and a copper pipe for heat extraction and (b) thermocouples drilled and inserted inside the LHTES tank

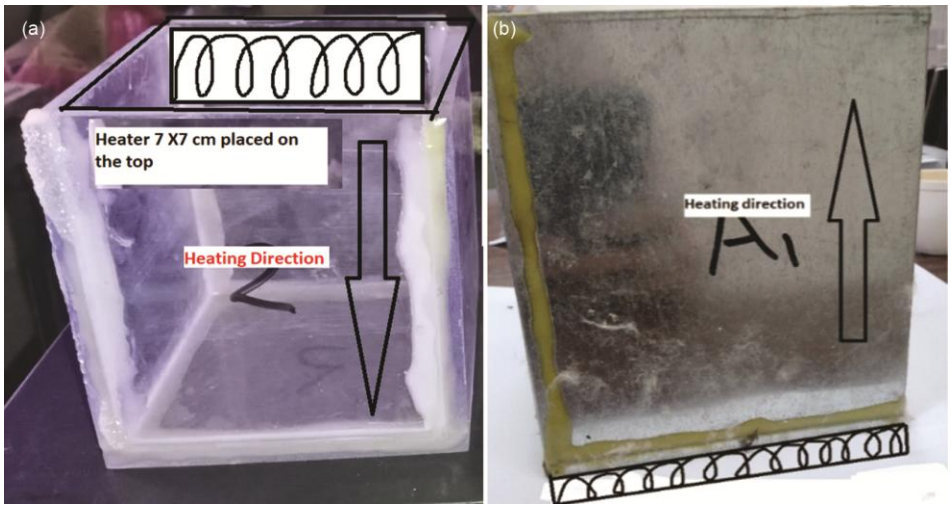

Figure 5 — The LHTES tank heater placement and heating direction (a) Heater placed on the top opening of the acrylic box (b) Heater placed at bottom of the GI sheet box

2.5 Methodology

Two types of heating were provided to the LHTES tanks during the experimental process. The heater was placed at the top opening present in the acrylic boxes and the heater was placed at the bottom in the case of the GI sheet box.

(A) Convective heating: A direct current (DC) power machine was used to produce the heat. The specifications of the DC heater were 300 V and 0.7 Ampere with a maximum power capacity of 120 Watts. The heater here was placed at the top of the encapsulated acrylic box and the heat transfer was from the top to the bottom of the box (Fig. 5(a)). There was a gap (2 cm) maintained between the heater and the wax-foam composite material to transmit the heat by convection. The box was covered with the help of glass wool so that the heat does not dissipate in to the environment. Simultaneously, all three thermocouples were properly connected to the data logger (Vernier Lab quest 2) to record the temperature of the wax at 1-minuteintervals. The DC power machine was run at a constant power of 30, 45, and 60 Watts.

(B) Conduction heating: The galvanized iron (GI) sheet box had the heater placed at the bottom of the box (Fig. 5(b)). The size of the heater was kept similar to convection heating (6.5 X 6.5 cm). The heater was in direct contact with the GI box base plate and conducted the heat directly to the foam-paraffin wax composite. The other heating conditions were similar to the convective heating process.

(C) Heat Recovering Process: When the entire wax melts in the box, the heat is stored by the wax in the form of specific heat and latent heat. The heat is also stored as the specific heat (aluminium) of the wire metal

foam and the copper pipe. The heat recovery setup is shown in Fig. 6(a & b). To recover this accumulated heat, we connect a plastic pipe for the water circulation on both ends of the copper pipe, after the melting process is completed. The water reservoir has 1 litre of water in the tank. Simultaneously, to understand the process of cooling the wax, the thermocouples also recorded the temperatures during the entire process of cooling. As water passes through the hot wax, heat is absorbed by it, and the temperature of the water rises which is noted with the help of software in the computer. After about 1 hour, the water temperature starts to stabilize due to thermal equilibrium. Therefore, after every hour the hot water is taken out and changed with 1 litre of cold water. In this way, cold water was changed for about 8 to 10 times. In this way, we find the efficiency of heat recovered from the system by experimenting with both the acrylic and GI metal sheet encapsulations.

2.6 Thermal conductivity, Thermo physical properties and uncertainty analysis

The thermo physical properties of the raw materials paraffin wax, copper foam, aluminium, and acrylic sheets are given below in Table 1[10].

The K-type thermocouples used during experiments have a tolerance of ± 0.2 ºC. The resistance of the heater wire was measured as approximately 138 and 11 **Ω** having a tolerance of ± 2 **Ω**. The calculation of uncertainty in the given electrical heat input, the uncertainty associated with voltage and current is ± 0.1 V and ± 1 mA as per the specification of the manufacturer. The heat lost from the heater was estimated at approximately 5-10 Watts assuming the natural convective heat transfer coefficient of air as 10 $W/m^2\,^{\circ}K$. The DC heater was estimated to have an error factor of approximately ± 15% on the output heat produced.

The thermal conductivity of the paraffin wax- wire woven composites was determined using the NETZSCH Hyper flash LFA 467 apparatus. The sample size was taken as 20 mm diameter and the thickness as 4 mm. The differential scanning calorimetry (DSC) was carried out on Mettler Toledo DSC1 for the paraffin wax samples.

3 Results and Discussion

3.1 DSC and thermal conductivity analysis of the aluminium wire foam structure- paraffin wax composites

Figure 7(a) shows the differential scanning calorimetry (DSC) study of the paraffin wax during the heating and cooling cycles. The DSC curve show two melting peaks at 42 °C and 60 °C and two peaks at 55 °C and 40 °C during the cooling of paraffin wax. This indicates that the wax starts to melt at 42 °C and the complete melting occurs around 60 °C. The thermal energy released by paraffin wax is calculated as 139 KJ/Kg during the cooling cycle and 158 KJ/Kg during the heating cycle.

Figure 7(b) shows the energy dispersive spectroscopy (EDS) of the aluminium metal wire. The elemental analysis of the wire was 97.17 wt % of Al and 2.83 wt % of Oxygen. The EDS showed the

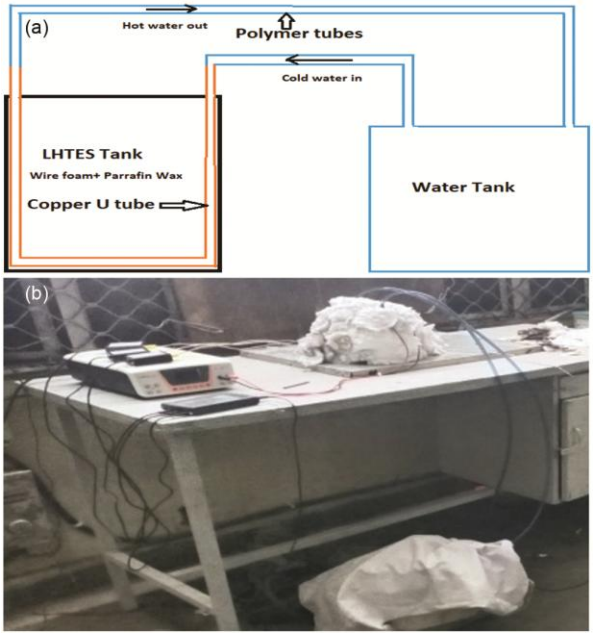

Figure 6 — The LHTES tank heat recovery process (a) set up diagram (b) experimental setup

Table 1 — Thermo physical properties of the raw materials

Material	Parameters	Values
Paraffin wax	Latent Heat (KJ/Kg)	185.8
	Density (Kg/m^3)	861
	Thermal conductivity (W/m°K)	0.4
	Specific heat capacity(KJ/kg° K)	2.14
	Melting temperature (°C)	60-62
	Viscosity at 65°C (MPa s)	6.01
Aluminium	Density (Kg/m^3)	270
	Thermal conductivity (W/m °K)	237
	Specific heat capacity(KJ/kg °K)	0.91
Acrylic	Thermal conductivity (W/m °K)	0.19
	Melting temperature (°C)	177
	softening temperature (°C)	110

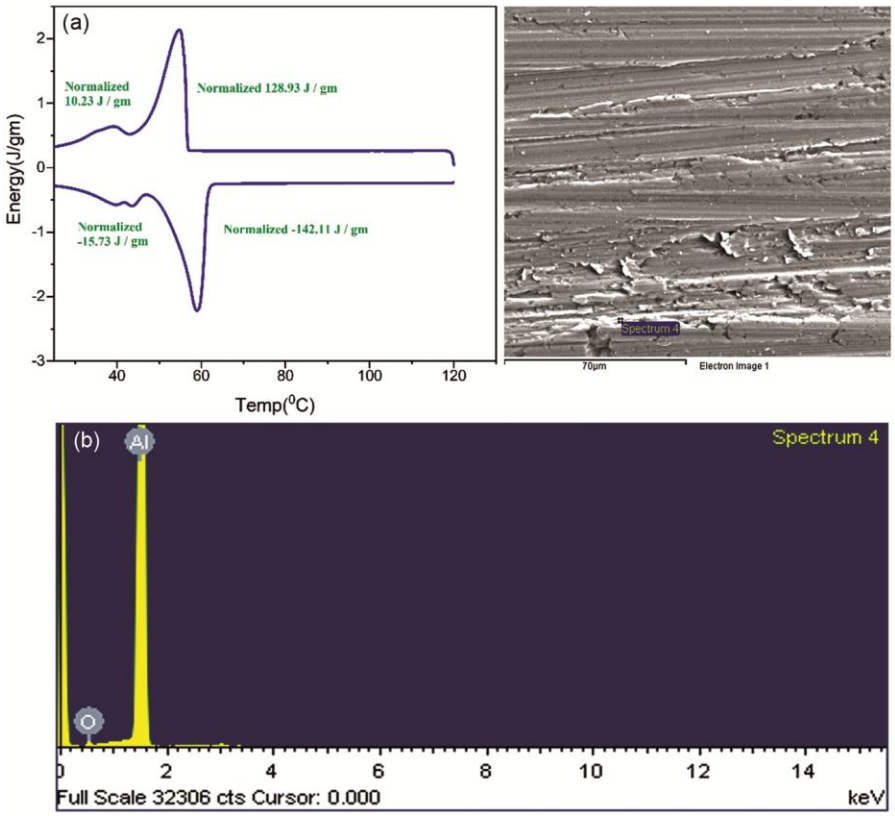

Figure 7 — DSC heating and cooling of pure paraffin wax showing total heat stored and released in paraffin wax and (b) EDS spectra of used aluminium wires

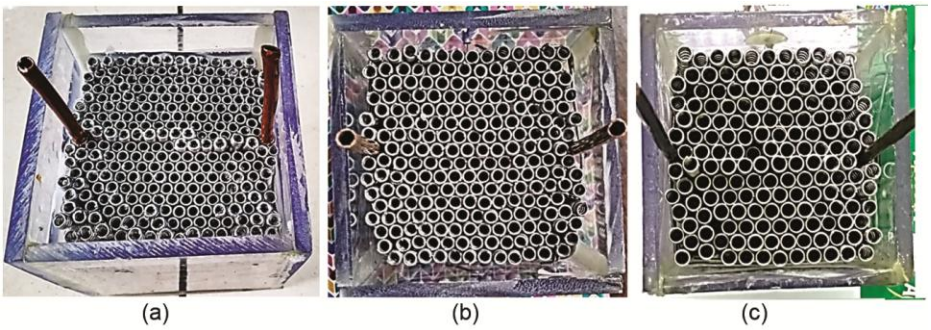

Figure 8 — Top view of the aluminium wire foam structures with (a) 4, (b) 5, and (c) 6 mm pore diameter

aluminium wire used in this study was pure with no other impurities.

Figure 8 (a-c) show the top view of the metal wire woven structures made from aluminium wires. The internal pore diameter was 4 mm, 5 mm, and 6 mm in each case respectively. The pores per square inch (PPI) of the wire woven structures were measured as 15, 12, and 9 for the 4, 5, and 6 mm pore diameters. The porosity obtained in 4, 5, and 6 mm pore diameters were 75.2 vol %, 78.5 vol %, and 83.5 vol % respectively. The number of metal wire springs reduced with the increase in the diameter of the springs. This leads to an increase in the porosity with increasing pore diameters.

Hu *et al.*[22] have reported that with a porosity of around 70 %, the thermal conductivity can be increased up to 123 times. The thermal conductivity reduces to 17 times when the porosity is increased to 95 %. Therefore, a lower porosity foam having a higher metal content is more beneficial in increasing the thermal conductivities of the metal foam-wax composites. Hence, lower porosity foams used in this study would be useful for obtaining better thermal conductivity of PCM.

In earlier works, high porosity foams have been used because it is difficult to infiltrate the wax in low porosity foams. It can be pointed out here that the filling of PCM in these wire foam structures was much easier due to the open structure of the wire-woven metal structures even at low porosity. Once the foam structures were formed, they were encapsulated with the help of an acrylic polymer sheet. Further, these Al-wire woven foam structures were filled with the phase change material i.e. paraffin wax by direct pouring the wax over the wire foams. Table 2 shows the weight of the aluminium structures, and the amount of wax added in each case. It can be observed that the amount of wax added was 31 % and 25 % higher in the case of the 6 mm wire foam structure compared to the 4 and 5 mm wire foam structures. The total weight of the encapsulated structure is maximum in 6 mm diameter foam structures due to the maximum amount of paraffin wax added in this case. Further, it is worth mentioning that, in earlier studies, metal foams with high porosities (> 90 vol %) and lower pore size (20-40 PPI) are used. This was because the metal foams need to be open cellular for the wax to infiltrate in the pores. However, this was not the case in our wire foams (9-15 PPI) which have a lot of open space due to their larger pores (4, 5, and 6 mm) and interconnected pores.

Table 2, also shows the values of the thermal conductivity measured for the 4, 5, and 6 mm samples using the NETZSCH Hyper flash LFA 467 apparatus. The samples show that the thermal conductivities have increased three to six times compared to the pure paraffin wax.

Table 3, shows a comparison of some of the earlier works[26-28] on metal foams and the subsequent increase in the thermal conductivity of paraffin wax. It can be observed that the thermal conductivity in our study is comparable to the nickel, and copper foams. The designed wire structures in this study are increasing the thermal conductivity at par with the open cellular copper and nickel foams. The wire foams are also providing the additional advantage of not obstructing the convective channels for heat transfer due to their convective design which was a limitation in earlier studies[29]. The pore sizes used in the present study are also fairly large *i.e.* 15, 12, and 9 PPI when compared with the earlier studies which have used 20-40 PPI foams.

Some authors[30,31] have also given some empirical relationships to calculate the theoretical thermal conductivities of metal foam-PCM composites. Bhattacharya *et al.*[30] have given an empirical correlation shown in equation 1.

$$ke = A\,(kf + (1-e)ks) + (1-A) \div \left(\frac{e}{kf} + \frac{(1-e)}{ks}\right) \quad \ldots (1)$$

Wherein; A= 0.35; e = total porosity in metal foam k_f = thermal conductivity of wax; k_s = thermal conductivity of the aluminium metal.

Table 2 — Various experimental input parameters in the wire woven foam structures - wax composite materials

S. No.	The internal diameter of spring structure (mm)	External diameter of spring structure (mm)	Box weight (gm)	Wire woven foam weight (gm)	Wax weight (gm)	Total box weight (grams)	Measured Thermal conductivity (W/m °K)	Metal/PCM ratio
1.	4	6.5	664	668	840	2172	2.279	0.79
2.	5	7.4	668	580	880	2128	1.297	0.65
3.	6	8.4	642	446	1102	2190	1.293	0.40

Table 3 — Effect of metal foam and wire-woven metal foams on the thermal conductivity of paraffin wax

S no.	Type of foam	Pore size (PPI)	Thermal conductivity (W/ m° K)	Increase in the thermal conductivity (times)	Ref No.
1.	Nickel foam	40	0.4768	1.8	[26]
2.	Copper foam	40	1.452	7.51	[26]
3.	Copper foam	20	1.238	4.1	[27]
4.	Copper foam	30	1.439	4.76	[27]
5.	Nickel foam	20	0.734	2.43	[27]
6.	Nickel foam	30	0.922	3.05	[27]
7.	Nickel foams	--	1.2	3	[28]
8.	Aluminium wire	15	2.279	5.69	Present study
	woven foams	12	1.297	3.23	
		9	1.293	3.24	

However, the theoretical values of the thermal conductivities obtained for our wire foam structures from Eq. 1 (21.1, 18.4, and 15.6 W/m°K) are much higher than the obtained experimental values. This suggests that the model used by various previous researchers may not be appropriate in our case of metal wire foams. The numerical simulation has been performed by assuming the pores as a hexagonal cell[30] or tetrakaidecahedral shape[31] which does not relate to the pore shape used in this study. The wire-woven metal foams have a new and simple design of a helical spring which can further be analysed for numerical simulation.

3.2 Heating of paraffin wax- Al wire foam composites (Convective Heating)

Figure 9(a-c) shows the melting of wax at different time intervals in 4 mm dia metal wire foams at a heating rate of 30 W (3000 W/mm^2). The melting is seen to progress in a zone-wise manner from one thermocouple section (T1) to the other sections near T2 and T3 thermocouples. After 300 minutes of heating,all the wax melted as also seen from Fig. 12 c.

On increasing the heating power to 45 W (4500 W/mm^2),the melting was completed in 200 minutes. The wax melted in 33 % lesser time compared to 30 W. In the case of the 60 W (6000 W/mm^2), the melting was the fastest and was completed in only 160 minutes. However, the top portion of the acrylic box showed some distortion due to heat. This has happened because of the larger heat built up at the top portionof the acrylic box (near the heater), because of the high heat transferrate at 60 W. In an acrylic box, since the wax is heated from the top of the box it is important to take care of the following points during the experiment.

(a) The amount of wax should be taken in such a way that the level of the wax remains below the level

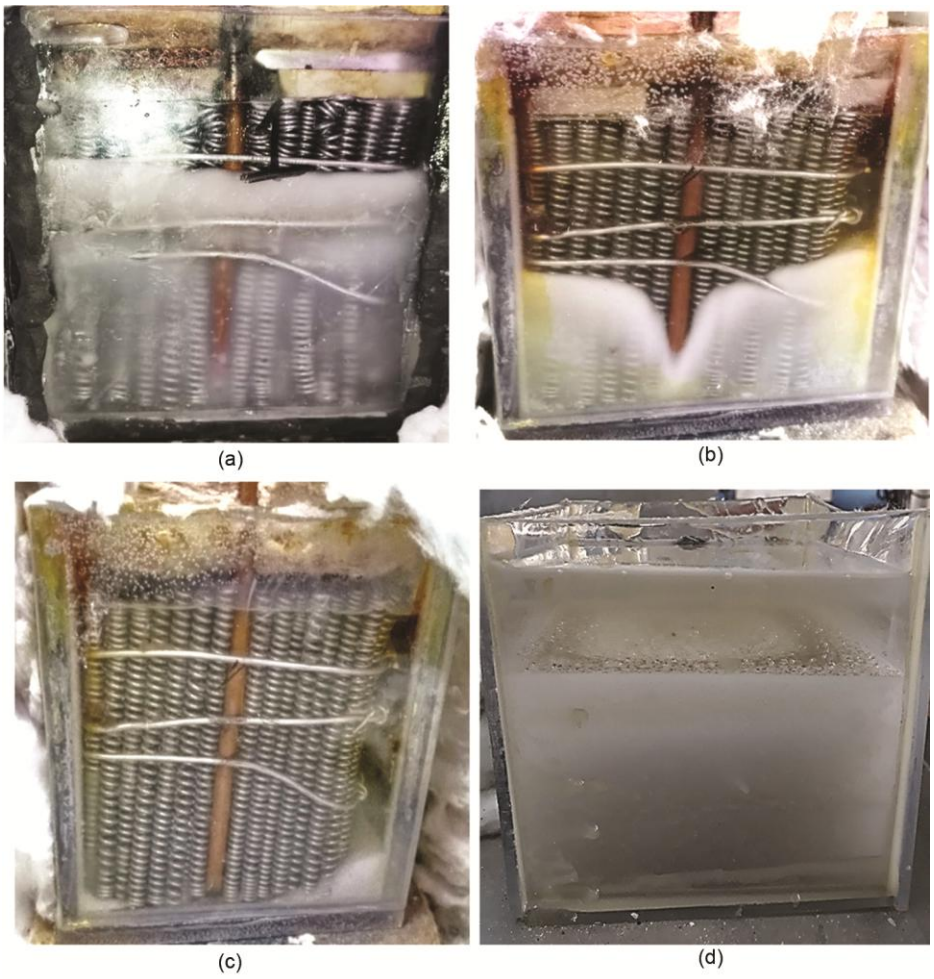

Figure 9 — The melting process in the acrylic box filled paraffin wax-4mm diameter wire metallic foams at 30 W (a) after 120 mins, (b) 170 mins, (c) 300 mins and (d) incomplete melting of paraffin wax without metal foam structure

of the metal foam structure upon melting. It was observed that during the melting process, the volume of the melted wax increases. The molten wax conceals the top portion of the metal wire structure. As a result, the metal wire structure does not get direct heat from the heater, due to which the heat cannot be conducted by the metal foam structure and it takes more time for the heat to reach the bottom. The melted wax tends to reflect more of the heat received from the source and acts as insulation. Due to this, the heat density starts to increase in the upper portion of the box, and the acrylic box starts to soften.

(b) The heater should generate heat at a reasonable rate

For smooth melting of wax in the acrylic box, the rate of heat supply should be kept in such a way that a balance is maintained between heat received and transfer. Due to this the box does not get distorted. The heater coil should be arranged in such a way that the heater coil spreads over the maximum metal foam structure so that the heat can reach the maximum wax quickly and the wax melts quickly. However, care should be taken to keep the heater away from the walls of the acrylic box to avoid its melting. As the wax melts from the top surface, the molten wax move upwards due to a decrease in its density, not downwards, so there is very little transfer of heat from the melted wax to the bottom. The transmission of heat to the bottom particles mostly takes place through the metal structure itself.

Figure 9(d) shows the effect of heating wax without any metal foam structure. It can be seen that there is heat built up on the top of the box and there was melting in the top portion only. Thereafter, the box gets deteriorated and the wax starts to burn off. This happened because the molten wax transmitted the heat very slowly due to its poor thermal conductivity. Hence, convective heating of wax was not possible without using metal foam structures.

Figure 10(a) shows the temperature recordings of the thermocouples at 30 W during the melting of paraffin wax. The graph indicates the temperature of the thermocouples inserted at a regular interval of 3 cm. It can be seen that the T1 thermocouple (near the heater) temperature increased rapidly during the initial 75 minutes. It suggests that the heat retention was more in the upper part of the acrylic box until the melting occurred near the T1 region. The heat started to transmit toward the bottom of the acrylic box after the paraffin wax had melted in the T1 region. Thermocouples 2 and 3 placed at an equal distance from thermocouple 1 show a rise of the temperature to 80 °C and 50 °C after 300 minutes. It can be inferred here that the heat transmitted from one zone to the other zone, only when the melting occurred in the subsequent upper zone. This leads to a conclusion that the heat gets transmitted more effectively by the molten wax through convection. During the convective heating, once melting starts at the heater end, convective channels should be present which can transmit the heat toward the bottom.

Figure 10(b) shows the effect of increasing the heating power to 45 W on the temperatures of the thermocouples. The temperatures of the T1 thermocouple reached 150 °C in 200 minutes. The temperature of the T2 thermocouple also shoots up to 100 °C upon increasing the heating power. However, it can be seen that the temperature of the T3 thermocouple did not rise much and was similar to the former case of 30 W. The spiral coiled springs are extending from the top to the bottom of the acrylic box and conduct the heat from the top to the bottom of the box. However, it is observed that only after the melting of wax in a particular zone, the heat is getting transferred toward the next zone. On increasing the heat transfer to the acrylic box, the heat gets accumulated on the top of the box, and only when the melting occurs the heat is transferred toward the

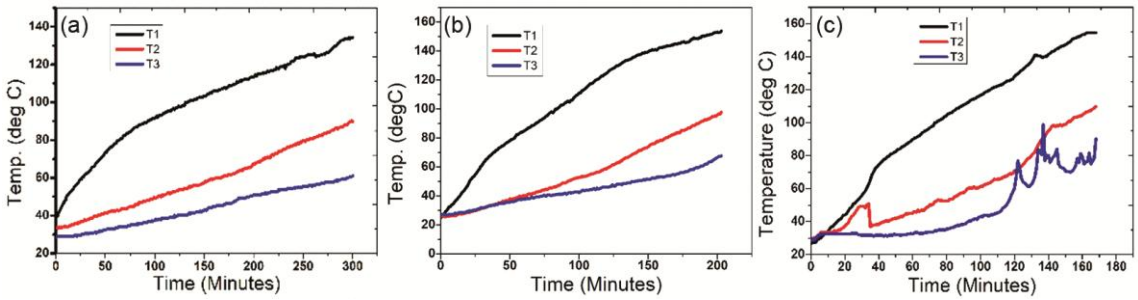

Figure 10 — The increase in the temperatures of the thermocouples after heating at different heating rates (a) 30 W, (b) 45 W and (c) 60 W

bottom regions of the wax. So, it is clear that convection plays a major role in transferring heat toward the bottom of the acrylic box. The conduction phenomenon is also playing a role in heat transfer but it is lesser than the convection process at 30 and 45 W.

Figure 10(c) shows the heating effect at a 60 W heating rate. Here, we can see that the T1 temperature has increased to 150 °C after 160 minutes. The T2 temperature also increased to more than 100 °C after 160 minutes. The temperature of the T3 thermocouple was the maximum in this case and was around 80 °C. It suggests that on increasing the input power to 60 W, the aluminium wire foam structure can transfer the high heat power at a much faster rate compared to 30 W and 45 W heating rates. This suggests that the metal wire foam structure is effectively transferring the heat from the top of the box toward the bottom regions of the box. Here, conduction becomes a major phenomenon wherein the spring structure quickly heats up and transmits the heat to the bottom of the acrylic box. Thus, it can be concluded here that the metal foam structure is more effective with an increasing rate of heat transfer. At a higher heat rate, the spring structure gets heated up rapidly due to its high thermal conductivity. This spring is extended from the top to the bottom and hence it heats up the wax in all the regions. At a lower heat transfer rate, the springs did not heat up as rapidly as at 60 Wand transferred heat majorly by convection.

3.3 Melting pattern in different Al wire foam structures

Figure 11(a-c) show the melting pattern obtained in the 4, 5, and 6 mm diameter foams at 30 W. The amount of melting in 300 minutes can be seen to be almost similar in all the cases. A little amount of unmelted wax is present in all cases after 300 minutes. However, as we know that the maximum amount of wax was present in the 6 mm diameter foams, it can be inferred that the maximum melting was obtained in 6 mm dia foams. The 6 mm dia foam structures also had approximately 33 wt. % lesser metal as compared to the 4 mm diameter foam structures. This leads to the conclusion that during convection heating, more openness of the structure (larger pore diameter) is essential for faster melting of wax. Also, a maximum amount of melting was obtained in the 6 mm diameter foam structures at 45 W convective heating (Fig. 12 (a-c)).

3.4 Repeatability of the Experiments

In order to establish the repeatability of the heating pattern, other sets of experiments were repeated to ascertain the heating trend. Table 4 shows the temperature of the thermocouples in other sets of experiments. The table shows that there is only a little difference between the temperatures of the thermocouples during the heating cycle. However, the final temperatures at the end of the heating cycle were found to be almost similar.

3.5 Heating cycle in GI metal encapsulation (Conductive Heating)

The experiments were further carried out in a GI sheet encapsulation for observing the effect of metal encapsulation on the melting of wax. Here, as explained in the experimental section the mode of heating is conduction. Fig. 13 shows the effect of heating wax at different heating powers in the 4 mm foam structures. The least time for melting was noted at 60 W and the maximum time for 30 W.

Table 5 shows the effect of the pore diameter on the total melting time required for the pure wax and

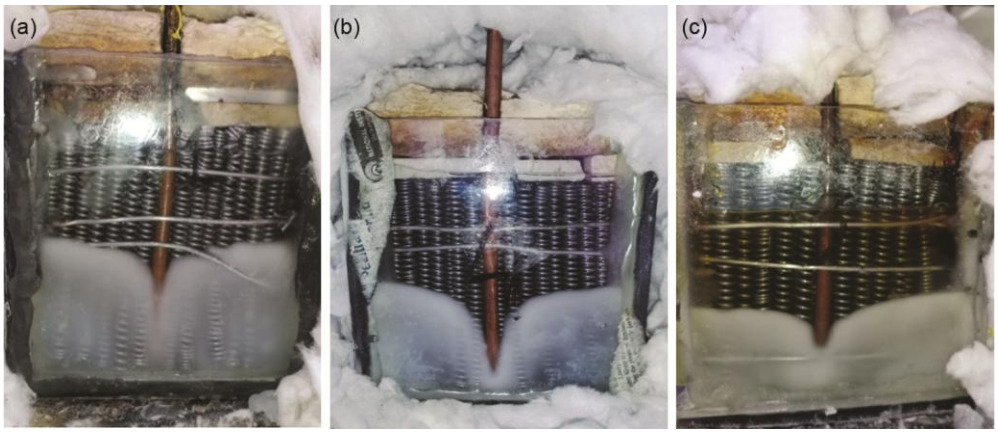

Figure 11 — The melting process in the acrylic box filled paraffin wax wire metallic foams at 30 W after 300 minutes, (a) 4 mm diameter foams (b) 5 mm diameter foams and (c) 6 mm diameter foams

Table 4 — The rise of the thermocouple temperatures during the heating cycle in different experiments

S.No	Time (in Min)	Al Structure-Acrylic Box - Heating Cycle					
		4 mm-Al Pore Size 30 W		5mm-Al 30 W		6mm-Al 30 W	
		Exp 1	Exp 2	Exp 1	Exp 2	Exp 1	Exp 2
1	0	33.2	29.0	27.8	23.5	27.7	27.6
2	15	34.4	29.4	29.0	25.7	28.9	29.0
3	30	37.5	30.6	31.0	27.4	32.0	32.1
4	45	40.2	32.9	34.1	30.2	34.4	36.7
5	60	42.2	35.7	37.6	31.0	37.9	40.2
6	75	44.6	39.6	40.0	34.0	41.0	46.4
7	90	47.7	43.9	42.3	36.4	53.1	50.0
8	105	50.4	46.2	44.3	39.1	58.2	55.1
9	120	52.8	46.4	46.6	41.9	59.4	57.8
10	135	55.5	47.4	48.6	43.8	61.7	61.7
11	150	57.4	49.0	51.7	46.5	64.5	64.4
12	165	60.2	52.1	53.3	48.8	66.8	66.9
13	180	62.1	58.4	55.6	52.1	68.8	68.7
14	195	65.2	62.6	58.4	54.4	73.8	73.9
15	210			61.9	57.9	78.1	78.2
16	225			65.0	61.5	82.4	82.5

Table 5 — Effect of pore diameters on the total time required for complete melting of wax at different heating power

S. No.	The pore diameter of the wire foams	Wax weight (grams)	Aluminium wire foam weight (grams)	Total time required for melting at different heating rates		
				30 W	45 W	60 W
1	--		--	600	540	325
1	4 mm	1064	668	292	178	128
2	5 mm	1002	580	324	196	145
3	6 mm	992	446	377	198	166

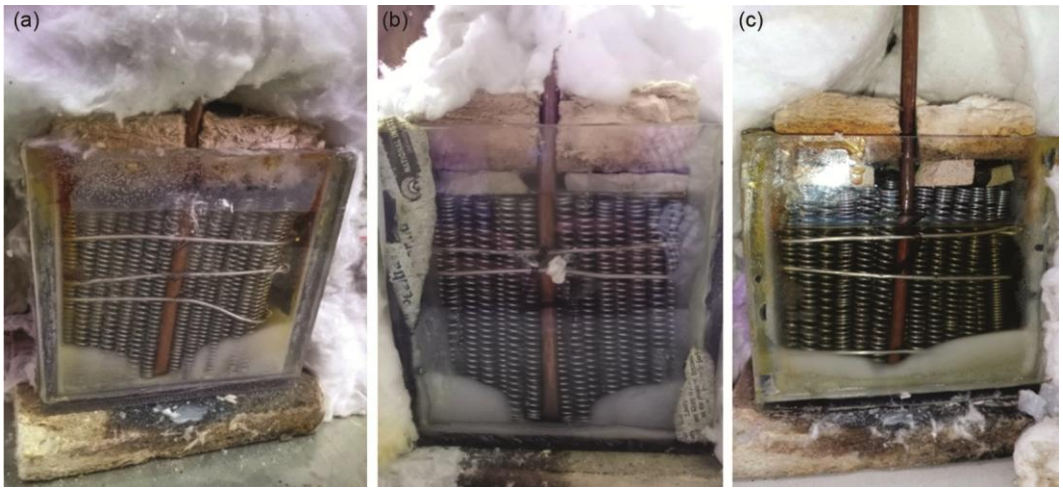

Figure 12 — The melting process in the acrylic box filled paraffin wax wire metallic foams at 45 W after 160 minutes, (a) 4 mm diameter foams (b) 5 mm diameter foams and (c) 6 mm diameter foams

the wax–metal wire foam composites. The time required for the melting of pure paraffin wax was the highest ranging from 300 to 600 minutes at 60 W and 30 W respectively. The melting of the wax in case of without using any metal structure progressed in the form of a vortex as can be seen in Fig. 14 (a & b) Even some wax was seen to be un-melted near the walls of the boxes even after 600 minutes of heating. This vortex formation was because of the heating area at the centre of the box (6.5 cm X 6.5 cm) compared to the cross-sectional area of the GI sheet box i.e. 10 cm X 10 cm. The heat is concentrated at the

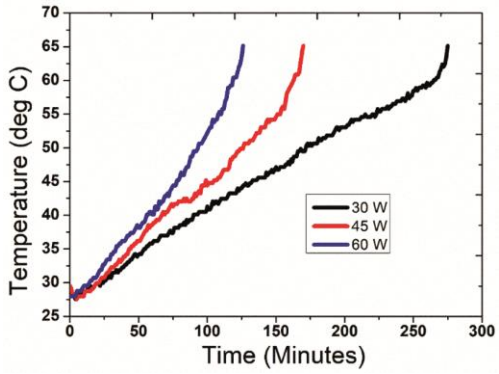

Figure 13 — The heating of the paraffin wax- wire foam composites through conduction heating showing total time required for the melting process

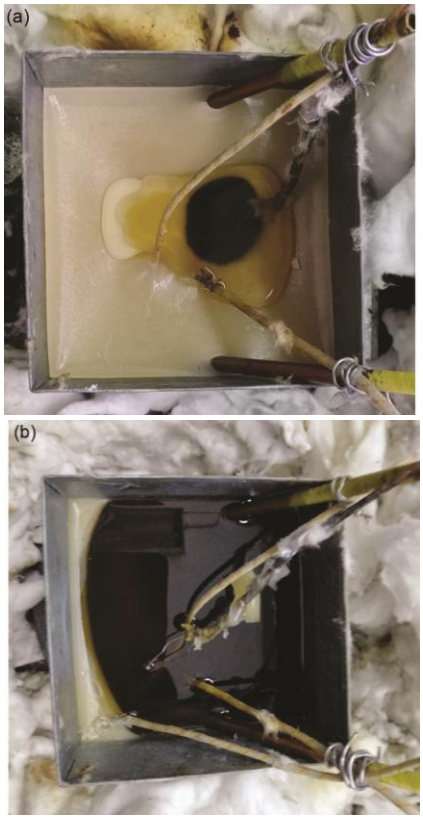

Figure 14 — The heating of the pure paraffin wax through conduction heating showing (a) vortex formation during melting and (b) wax present at the side walls after 600 mins at 30 W

central part of the box and the melting first occurred in the centre which led to the formation of such a vortex.

Further, we can see the total time required for the melting of wax-wire foam composites in the various foam structures. The melting was uniform and it did not progress in the form of a vortex as seen in the case of pure wax. The time taken for the melting is the least in the case of the 4 mm wire foams. The total

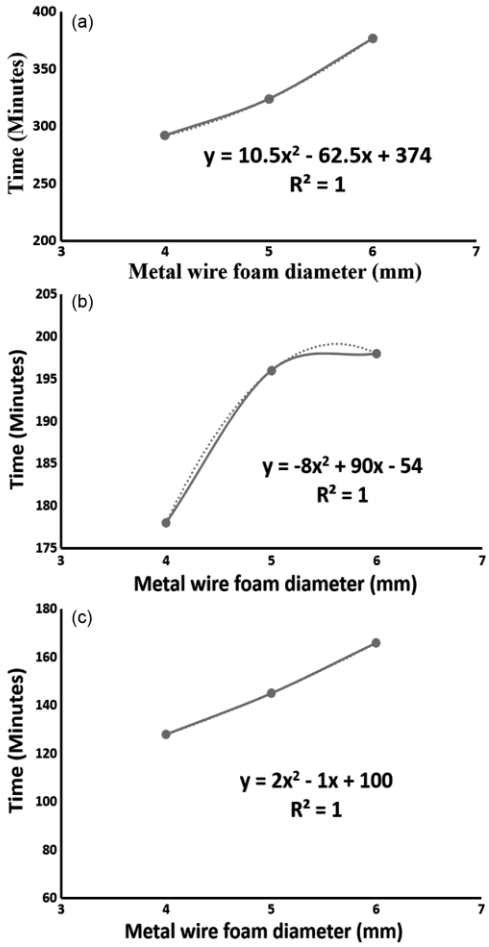

Figure 15 — The total time required for melting of paraffin wax plotted with respect to the different pore diameters (a) 30 W, (b) 45 W, and (c) 60 W

time for melting increased, as we increase the diameter of the pores. The results have also been plotted and the equations have been calculated for finding out the effect of an increase in pore diameters on the total time required for melting. Fig. 15(a-c) show the trend lines plotted for the melting time as a polynomial function of the pore diameter at various heating rates. The R-squared values of all the cases are equal to 1 which suggests good experimental values obtained during the experiments. These equations can be beneficial to find out the total time required at different heating rates and different pore diameters of the wire foams.

The results as well as the equations show that with the increasing pore diameters, the time required for the melting of the wax also increases. These results are contrary to the earlier results obtained during convective heating. During conduction heating, heat transfer takes place through metal foam structures.

Therefore, the 4 mm diameter foam structures had the fastest melting, and the slowest melting was obtained for the 6 mm diameter foams. However, during convective heating, 6 mm diameter foam structures had the fastest melting when the heating mode was convective. Hence, it can be inferred that in the case of convective heating, the heat transfer is mostly through convection and larger diameter foams are more beneficial. On the contrary, smaller diameter pore structures are more beneficial when the heating is done in the conduction mode.

3.6 Heat extraction

The water circulation method was used to extract the stored thermal energy from the molten wax placed in the acrylic and the GI sheet encapsulations. This was done by placing a copper "U" shaped tube with 4 mm and 6 mm internal and external diameters touching the walls of the encapsulating containers. The copper tube has been bent in the form of a "U" shape such that its two ends are at the top. The length of the two arms of a U shape is approximately 15 cm, and cold water was circulated for an hour. After which the hot water was removed from the vessel and again 1 litre of cold water is taken. In this way, the heat was recovered for 6 to 8 cycles. During the experiment, it was found that when water is passed through thermal storage for one hour, the temperature of the water increases rapidly during the initial 30 minutes. However, as the temperature of water increases, the temperature difference between molten wax and water decreases. So after each cycle, the water absorbs lesser heat than the previous cycle. And after about 45-50 minutes, when the temperature of the water reaches a steady state, water starts to extract very little heat. Therefore, in these circumstances, after a steady state is reached the hot water is replaced by cold water. It was also observed that, if the same water is continuously circulated through the thermal storage, then the temperature is almost constant for a long time, for about 12-15 hours. It can be inferred here that, if the temperature of a fixed volume of water is to be kept constant, then we must circulate the same water through thermal storage. This application can be very useful for keeping the temperature of a certain volume of water constant for a long duration in cold regions.

Table 6 shows the various heat extraction cycles of the water showing the increase in the temperature of the water after every cycle. The heat extraction continued for 9-10 cycles and there is a constant decrease inthe outlet temperature of the water with each cycle. The heat extraction was continued for 9 cycles in the 4 mm diameter foam structures. The heat extraction was stopped when the outlet temperature difference was reduced below 7 °C. The heat extraction in 5 mm foam structures continued for 10 cycles and the temperature difference after the 10^{th} cycle remained above 7 °C. The heat extracted was also the maximum in this case. The heat extraction in 6 mm diameter foams could continue for 9 cycles. These results show that the heat extraction was more uniform and maximum in the 5 mm diameter foams and the peak temperature gradually decreased with each heat extraction cycle. The heat extraction of 396.1 kJ was also found to be the maximum in this case.

Figure 16 shows the decrease in temperatures of the thermocouples during the extraction of heat from the acrylic box-encapsulated molten wax–wire foam composites. The T1 thermocouple is attached at the top of the box, T2 in the middle portion, and T3 at the

Table 6 — Heat extraction and rise in temperature of water during each cycle

Cycle No.	Time Duration, minutes	Increase in the water temperature after passing LHTES, in different Al-wire foam structures (Acrylic sheet encapsulation)		
		4mm	5mm	6 mm
01	0-60	15.7	16.3	15.3
02	60-120	9.8	10.7	9.4
03	120-180	8.4	9.6	9.3
04	180-240	8.7	9.3	8.2
05	240-300	7.7	9.5	8.1
06	300-360	7.1	8.7	7.4
07	360-420	6.6	7.9	7.3
08	420-480	6.4	7.5	7.1
09	480-540	6.4	7.5	7.0
10	540-600	--	7.3	6.6
	Total energy extracted, kJ	322.6	396.1	359.9

base of the box. They show that the temperatures of the thermocouples begin to decrease as soon as the water starts to flow in the copper U tube. The copper tube is in direct contact with the three walls (one base wall and the other two side walls) of the container. The thermocouples are attached to the opposite walls of the copper tube. It can be expected that the temperature of the T1 will fall more rapidly followed by T3 and T2 thermocouples. This trend was seen in the 4 mm diameter wire foams. T1 thermocouple temperature has dropped rapidly in the first 50 minutes of heat extraction. It can also be noted that the temperature of the thermocouple T2 did not decrease and remained more than 60°C even after 600 minutes. This suggests that the heat has got trapped in the central part of the box and is not getting transferred to the base or sides of the container.

Figure 16(b), shows the cooling trend in the 5 mm diameter foams wherein there is a uniform decrease in temperature of all the thermocouples. This suggests that the heat has got extracted from all the sections of the box uniformly. In the case of 6 mm (Fig. 16(c)), the heat is lost rapidly from the top of the box (T1). The temperature of the T2 thermocouple in the middle part remained high till 480 min. this suggests that the heat extraction from the middle portion was stagnant. This has happened because the T1 region lost heat rapidly due to the larger diameter pores. Similarly, the bottom region of the box also lost heat rapidly to water. This led to the solidification of wax in the top and bottom regions of the box. Hence, the heat became entrapped in the middle portion of the box. Thus, having a very larger pore size released the heat more rapidly due to its high convective area, and uniform heat extraction was not accomplished. It can be seen that the temperatures T1, T2, and T3 are reducing continually in the case of the 5 mm diameter pore wire foams (Fig. 16(b)). The graph also shows that the T2 temperature had the maximum decrease in its final value in this case. Thus, on comparing all the results we can see that the 5 mm was an ideal pore diameter wherein the heat extraction was complete and uniform from all parts of the container.

Table 7 shows the heat extraction cycles from the GI sheet box encapsulated molten wax–wire foam composites. Here, we can see that the number of cycles has reduced compared to the earlier case of acrylic box encapsulation. It suggests that the heat has been lost from the GI sheet box considerably. The number of cycles is the least in the case of the 4 mm diameter foams. This was because of the highly

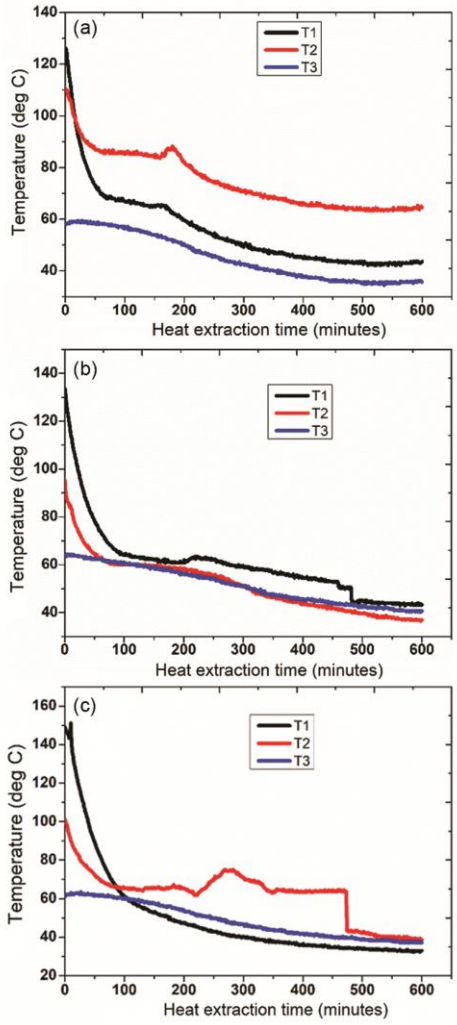

Figure 16 — The decrease in the thermocouples (T1, T2, and T3) temperature during the heat extraction (a) 4 mm, (b) 5 mm, and (c) 6 mm wire foam structures

conductive nature of the 4 mm diameter foams compared to others, which have lost more heat to the environment. The 5 mm diameter foam structures show a smooth decrease in the exit water temperature. The decrease in maximum peak temperature is more in the 6 mm diameter foams, suggesting lower heat extraction in later cycles. Hence, it may be inferred that GI sheet metal encapsulation has a higher heat loss to the environment and proper acrylic encapsulation has to be ensured in addition to the glass wool insulation for better thermal efficiencies.

3.7 Thermal efficiencies of the LHTES system

The total heat present in the LHTES system will be the sensible and latent heat of the paraffin wax. There will also be some heat stored in the aluminium spirals due to their sensible heating. The total heat given to

Table 7 — Heat extraction and rise in temperature of water during each cycle

Cycle No.	Time Duration, minutes	Increase in the water temperature after passing LHTES, in different Al-wire foam structures (GI sheet encapsulation)		
		4mm	5mm	6 mm
01	0-60	16.9	18.8	19.4
02	60-120	11.2	11	10.8
03	120-180	10.6	11	10.8
04	180-240	9.7	10.4	10
05	240-300	8.5	9.3	8.8
06	300-360	7.8	8.6	8.7
07	360-420	--	8.1	8.5
	Total energy extracted, kJ	271.7	324.2	323.4

Table 8 — Thermal efficiencies of the Aluminium wire foam–wax composites with acrylic encapsulation

Wire foam diameter (mm)	Heat Produced by Heater during the cycle@30WattKJ or J/cm^3	Total Absorbed Heat by System, KJ or J/cm^3	Total Extract Heat, KJor J/cm^3	Efficiency with Wax (Absorb Heat)	Efficiency with Heater (Produce Heat)
4	540	416.2	322.6	77.5	59.7
5	590.4	428.3	396.1	92.5	67.1
6	604.8	533.6	359.9	67.5	59.5

the LHTES system can also be calculated by the heater power rating and its total working time. The extracted heat was calculated for each water circulation cycle from its sensible heat stored.

The thermal efficiency was calculated by the following general formulas:

The total heat content of the encapsulated box

Sensible heat of wax $S1 = m\,wax \times c\,wax \times \Delta t$ ... (2)

Sensible heat metal foam structure $S2 = m\,(metal\,foam) \times c\,metal \times \Delta t$ ... (3)

Latent Heat Energy $L1 = m\,wax \times L$ ... (4)

The total energy stored in the LHTES $Qs = S1 + S2 + L1$ ... (5)

Wherein: m is mass; c: specific heat capacity;

Total heat given by heater

Heat input by heater $H = P \times t$ ... (6)

Wherein: P: Power of heater; t: time in secs

Energy extraction

Energy extracted by Water $Qe = m\,water \times c\,water \times \Delta T$ ... (7)

The thermal efficiency of the LHTES system is calculated concerning the heat stored in LHTES as

$\eta = (Qe \div Qs) \times 100$ ... (8)

The thermal efficiency of the LHTES system is calculated concerning the heat given by the heater as

$\eta = (Qe \div H) \times 100$ ... (9)

Table 8 gives the thermal efficiency of various wax and wax-foam composite LHTES systems concerning the energy stored and energy supplied by the heater. The thermal efficiencies were the highest in the 5 mm diameter foams. This result is in accordance with the previous results wherein the temperature of all the thermocouples was reduced to the lowest in all the cases. In Fig. 16(b), we had seen that the 5 mm diameter foams had the best heat extraction. This suggests that both convective and conductive structure is required for better thermal efficiencies. The thermal efficiency was the lowest in the 4 mm diameter foams. This shows that the smaller pores and a larger amount of the metal did not affect the thermal efficiency. On the other hand, the thermal efficiency of the system improved when the size of the pores was increased to 5 mm. However, with a further increase in the pore diameter to 6 mm the efficiency decreased because of the faster heat transmitted to the water during the process.

The thermal efficiencies were also more in the 5 mm diameter wire foams-wax composites using the GI metal encapsulations (Table 9). The heat content was the maximum in the 6 mm diameter wire foam–wax composites due to the maximum amount of wax present in these foams. However, the heat extraction was lesser than the 5 mm diameter wire foams. This suggests that in this study 5 mm diameter wire foam's thermal performance was also the best due to its combined convective and conductive properties.

Table 9 — Thermal efficiencies of the Aluminium wire foam–wax composites with GI sheet encapsulation

Wire foam diameter (mm)	Heat Produced by Heater during the cycle @60WattKJ or J/cm^3	Total Absorbed heat by System KJ or J/cm^3	Total Extract Heat KJ or J/cm^3	Efficiency with Wax (Absorb Heat)	Efficiency with Heater (Produce Heat)
4	568.8	373.3	271.7	72.8	47.8
5	640.8	412.5	324.2	78.6	50.6
6	712.8	426.5	323.4	75.8	45.3

4 Conclusion

1 Lightweight Aluminium wire woven metal foams are a new and economical way to design convective designed metal structures for increasing the thermal conductivity of the organic phase change materials like paraffin wax.

2 Even low-porosity metal wire foam can have a highly open structure with high thermal conductivity and be easily fabricated to make the LHTES.

3 The heat was transmitted more effectively in the larger diameter foams when the heating mode was kept as convection and the trend reversed when the heating mode was changed to conduction.

4 The effect of using a polymer (acrylic),and a galvanized iron (GI) sheet showed that the acrylic encapsulation helped in better heat retention and obtaining higher thermal efficiencies.

5 The heat extraction continued for a longer number of cycles in the 5 mm diameter foam-wax composites. The heat extraction was also uniform and the heat was extracted from all parts of the LHTES. The thermal efficiencies were also higher for the 5 mm diameter foams when compared to the 4 mm and 6 mm diameter foams due to better heat extraction.

6 The convective-designed wire foams with circular pores can be an effective solution for increasing the thermal conductivity of the phase change materials. The wire can also be designed in various other shapes easily and it is much easier to infiltrate them with the PCM. The above system can be used for various solar thermal energy storage applications.

Acknowledgment

The first author Mr Anup Kumar Khare, PhD Scholar gives his heart full thanks to the Director, CSIR–AMPRI, Bhopal for allowing his thesis work at AcSIR–AMPRI, Bhopal and for the experimental facilities used in this study. The authors also acknowledge the DSC facility provided by Dr Muhd. Shafeeq M.

References

1 Nazir H, Batool M, Osorio F J B, Isaza-Ruiz M, Xu X, Vignarooban K, Phelan P & Inamuddin K A M, *Inter J Heat Mass Trans*, 129 (2019) 491.

2 Sharma S D & Sagara K, *Inter J Green Energy*, 2 (2005) 1.

3 Sharma R K, Ganesan P, Tyagi V V, Metselaar H S & Sandaran S C, *Energy Convers Manag*, 95 (2015) 193.

4 Gil A, Medrano M, Martorell I, Lázaro A, Dolado P, Zalba B & Cabeza L F, *Renew Sustain Energy Rev*, 14 (2010) 31.

5 Oró E, Gracia A De, Castell A, Farid M M & Cabeza L F, *App Energy*, 99 (2012) 513.

6 Du K,Calautit J, Wang Z, Wu Y & Liu H, *App Energy*, 220 (2018) 242.

7 Yan T, Wang R Z, Li T X, Wang L W & Fred I T, *Renw Sustain Energy Rev*, 43 (2015) 13.

8 Ye H, Long L, Zhang H & Zou R, *App Energy*, 113 (2014) 1118.

9 Xu B, Li P & Chan C, *Appl Energy*, 160 (2015) 286.

10 Prasanth N, Sharma M, Yadav R N & Jain P, *J Energy Stor*, 32 (2020) 101990.

11 Ali M A, Fayaz, Viegas R F, Kumar M B S, Kannapiran R K & Feroskhan M, *J Energy Stor*, 26 (2019) 100982.

12 Yang X, Yu J, Xiao T, Hu Z & He Y, *Appl Energy*, 261 (2020) 114385.

13 Ibrahim N I, Al–Sulaiman F A, Rahman S, Yilbas B S & Sahin A Z, *Renew Sustain Energy Rev*, 74 (2017) 26.

14 Yang X, Niu Z, Bai Q, Li H, Cui X & He Y L, *Appl Ther Eng*, 161 (2019) 114163.

15 Selvam L & Ramalingam D, *J Braz Soc Mech Sci Eng*, 41 (2019) 572.

16 Chen J, Yang D, Jiang J, Ma A & Song D, *Proc Mater Sci*, 4 (2014) 389.

17 Siahpush A, O'Brien J & Crepeau J, *J Heat Trans*, 130 (2008) 082301.

18 Fleming E, Wen S, Shi L & Silva A K, *Inter J Heat Mass Trans*, 82 (2015) 273.

19 Zhu C Q, Ran F M & Fang G Y, *J Energy Stor*, 27 (2020) 101163.

20 Joshi V & Rathod M K, *J Energy Storage*, 22 (2019) 270.

21 Yang X, Wei P, Xinyi W & He Y L, *Appl Energy*, 268 (2020) 115019.

22 Hu X & Gong X, *Appl Therm Eng*, 151 (2019) 231.

23 Zhang L, Zhou K, Wei Q, Ma L, Ye W, Li H, Zhou B, Yu Z, Lin C T, Luo J, Gan X, *Appl Energy*, 233 (2019) 208.

24 Kang K J, *Prog Mater Sci*, 69 (2015) 213.

25 Zhao C Y, *Inter J Heat Mass Trans*, 55 (2012) 3618.

26 Huang X, Lin Y, Alva G & Fang G, *Sol Energy Mater Sol Cells* 170 (2017) 68.
27 Shang B, Hu J, Hu R, Cheng J & Luo X, *Inter J Heat Mass Trans*, 125 (2018) 596.
28 Jianqing C, Yang D, Jiang J, Ma A & Song D, *Proc Mater Sci*, 4 (2014) 369.
29 Venkateswarlu K & Ramakrishna K, *J Braz Soci Mech Sci Eng*, 44 (2022) 6.
30 Bhattacharya A, Calmidi V V & Mahajan R L, *Inter J Heat Mass Trans*, 45 (2002) 1017.
31 Xiao X, Zhang P & Li M, *Inter J Ther Sci*, 81 (2014) 94.